Published in final edited form as:
Gastroenterology. 2014 January ; 146(1): 245–256. doi:10.1053/j.gastro.2013.09.050.

DCLK1 Marks a Morphologically Distinct Subpopulation of Cells with Stem Cell Properties in Pre-invasive Pancreatic Cancer

Jennifer M. Bailey[1,2], **Janivette Alsina**[1], **Zeshaan A. Rasheed**[3], **Florencia M. McAllister**[3], **Ya-Yuan Fu**[5], **Ruben Plentz**[6,7], **Hao Zhang**[4], **Pankaj J. Pasricha**[5], **Nabeel Bardeesy**[6], **William Matsui**[3], **Anirban Maitra**[8], and **Steven D. Leach**[1,2]

[1]Department of Surgery, Johns Hopkins University School of Medicine, Baltimore, MD, 21205, USA

[2]The McKusick-Nathans Institute of Genetic Medicine, Johns Hopkins University School of Medicine, Baltimore, MD, 21205, USA

[3]Department of Oncology, Johns Hopkins University School of Medicine, Baltimore, MD, 21205, USA

[4]Department of Molecular Microbiology and Immunology, Bloomberg School of Public Health, Baltimore, MD, 21205, USA

[5]Department of Medicine, Johns Hopkins University School of Medicine, Baltimore, MD, 21205, USA

[6]Department of Medicine, Massachusetts General Hospital Cancer Center, Harvard Medical School, Boston, MA, 02114

[7]Department of Internal Medicine, Medical University Hospital, Tuebingen, Germany

[8]Department of Pathology, The Sol Goldman Pancreatic Cancer Research Center, Johns Hopkins University School of Medicine, Baltimore, MD, 21205, USA

Contact: Steven D. Leach, stleach@jhmi.edu.

Jennifer M. Bailey has no Conflict of interest
Janivett Alsina has no Conflict of Interest
Zeshaan A. Rasheed has no Conflict of Interest
Ya-Yuan Fu has no Conflict of Interest
Ruben Pletz has no conflict of Interest
Florencia McAllister has no Conflict of Interest
Hao Zhang has no Conflict of Interest
Nabeel Bardeesy has no conflict of interest
Pankaj Pasricha has no Conflict of Interest
William Matsui has no Conflict of Interest
Anirban Maitra has no Conflict of Interest
Steven Leach has no Conflict of Interest

SUPPLEMENTAL INFORMATION

Supplemental Information includes supplemental experimental procedures, five figures, two tables and one supplemental movie.

Author Contributions: J.M.B. participated in study concept, study design, data acquisition, data interpretation and manuscript preparation. J.A., Z.R., Y.F., F.M.M. and H.Z. participated in the acquisition of data. P.J.P., N.B. and R.P. provided material support; W.M. and A.M. provided important intellectual support, S.D.L. participated in study concept and design, study supervision, data interpretation and manuscript preparation. J.M.B. and S.D.L. obtained funding.

Abstract

Background & Aims—As in other tumor types, progression of pancreatic cancer may require a functionally unique population of cancer stem cells. Although such cells have been identified in many invasive cancers, is not clear whether they emerge during early or late stages of tumorigenesis. Using mouse models and human pancreatic cancer cell lines, we investigated whether pre-invasive pancreatic neoplasia contains a subpopulation of cells with distinct morphologies and cancer stem cell-like properties.

Methods—Pancreatic tissue samples were collected from the KC^{Pdx1}, KPC^{Pdx1}, and KC^{iMist1} mouse models of pancreatic intraepithelial neoplasia (PanIN) and analyzed by confocal and electron microscopy, lineage tracing, and fluorescence-activated cell sorting. Subpopulations of human PDAC cells were similarly analyzed and also used in cDNA microarray analyses.

Results—The microtubule regulator DCLK1 marked a morphologically distinct and functionally unique population of pancreatic cancer-initiating cells. These cells displayed morphologic and molecular features of gastrointestinal tuft cells. Cells that expressed DCLK1 also expressed high levels of ATAT1, HES1, HEY1, IGF1R, and ABL1, and manipulation of these pathways in PDAC cell lines inhibited their clonogenic potential. Pharmacologic inhibition of γ–secretase activity reduced the abundance of these cells in murine PanIN, in a manner that correlated with inhibition of PanIN progression.

Conclusions—Human PDAC cells and pancreatic neoplasms in mice contain morphologically and functionally distinct subpopulations that have cancer stem cell-like properties. These populations can be identified at the earliest stages of pancreatic tumorigenesis, and provide new cellular and molecular targets for pancreatic cancer treatment and/or chemoprevention.

Keywords

PanIN; Kras; Notch; acetylated tubulin

INTRODUCTION

Normal human tissues are characterized by hierarchical precursor/progeny relationships between resident stem cells and their differentiated offspring. Similar relationships may also exist in malignant human tumors, with unique subpopulations of “cancer stem cells” or “tumor-initiating cells” thought to be responsible for tumor maintenance. Several recent studies involving formal *in vivo* lineage tracing have confirmed the critical role played by cancer stem cells in multiple primary tumor types[1–3]. With respect to pancreatic cancer, subpopulations of cells with tumor-initiating capacities have been identified in human pancreatic cancer cell lines as well as in primary xenografts of human pancreatic ductal adenocarcinoma (PDAC)[4–7]. However, the role of stem cell populations in the maintenance and progression of *pre-invasive* pancreatic cancer (pancreatic intra-epithelial neoplasia; PanIN) remains unknown. In addition, while cancer stem cell populations have typically been distinguished based on unique patterns of cell surface marker expression, no information is available regarding whether or not these cells can be morphologically distinguished from their non-stem cell neighbors. To address these issues, we have examined the temporal onset of cellular and functional heterogeneity in early pancreatic cancer. These studies have revealed a novel and morphologically distinct tumor-initiating pancreatic cancer cell type, marked by expression of *Doublecortin and* Ca^{2+}*/Calmodulin-Dependent Kinase-Like 1* (Dclk1). These findings suggest that cellular heterogeneity and functional diversity represent defining features of both invasive and pre-invasive pancreatic cancer.

MATERIALS AND METHODS

All animal experiments described herein were approved by Johns Hopkins University Institutional Animal Care and Use Committees.

Mouse lines

The following murine models of pancreatic intraepithelial neoplasia (mPanIN) and invasive cancer were utilized: KC^{Pdx1}, KPC ^{Pdx1} and KC^{iMist1}. Each model utilizes Cre recombinase (C) to activate oncogenic *Kras*^{G12D} (K), either during development or in adulthood. The KC^{Pdx1} and KPC ^{Pdx1} models utilize a Pdx1:Cre allele to activate oncogenic Kras (KC^{Pdx1}) in embryonic pancreatic progenitor cells, either alone (KC^{Pdx1})[8] or in combination with inactivation of a floxed p53 allele (KPC ^{Pdx1})[9]. In contrast, the KC^{iMist1} model uses an inducible Mist1:CreER^{T2} driver line to activate oncogenic Kras in adult acinar cells[10]. Both models lead to the induction of pancreatic "ductal" neoplasia, with the progressive accumulation of mPanIN occurring over several months. For the KC^{iMist1} model, mPanIN formation was further accelerated by the induction of associated chronic pancreatitis using cerulein (Figure 1A–F). For experiments requiring either lineage tracing or fluorescence-activated cell sorting (FACS), selected KC^{iMist1} mice were also crossed onto either the either the Rosa26:LSL-YFP Cre reporter line (Y) or the Rosa26:loxP-membrane tdTomato-loxP-membrane GFP (mTmG) Cre reporter line (G), generating KC^{iMist1}Y mice and KC^{iMist1}G mice, respectively (Figure 1F).

Microarray analysis

$AcTub^{HI}$ and $AcTub^{LO}$ human PDAC cells were FACS sorted and RNA was isolated using the Qiagen RNeasy Isolation Kit. cDNA microarrays were performed using Agilent Human GE 4x44K arrays, with analysis of differentially expressed genes performed as previously described[11].

Clonogenic assays

FACS-sorted murine PanIN and human PDAC cell populations were subjected to clonogenic sphere-forming assays as previously described[12].

Additional detailed descriptions of all materials and experimental methods are provided in supplementary material.

RESULTS

A subpopulation of cells containing high levels of Dclk1 and acetylated-αTubulin are present in murine PanIN

In a survey of markers identifying unique PanIN cell subpopulations, we examined expression of acetylated α-Tubulin (AcTub) in mPanIN. Using immunofluorescent labeling, we characterized the prevalence and distribution of AcTub expressing cells in both KC^{iMist1} and KC^{Pdx1} mouse pancreas. While AcTub expression was observed in association with primary cilia in normal ductal epithelium and in areas of acinar-to-ductal metaplasia (ADM), we found no evidence of AcTub labeling of primary cilia in mPanIN epithelium (Figure S1A), consistent with the previously reported absence of primary cilia in these lesions[13]. However, we did observe a low abundance cell population in mPanIN epithelium containing high levels of both cytoplasmic and apical AcTub (Figure 2A), reminiscent of gastrointestinal tuft cells[14–17]. To further clarify the identity of AcTub positive PanIN epithelial cells, we performed double-labeling for AcTub and *Doublecortin and Ca*$^{2+}$*/Calmodulin-Dependent Kinase-Like 1* (Dclk1), a tuft cell marker previously reported to regulate epithelial-mesenchymal transitions in pancreatic cancer cells[18]. Using

immunofluorescenct confocal imaging, we observed a high degree of overlap between Dclk1 and AcTub expression in ADM and early mPanIN lesions from both KC^{iMist1} and KC^{Pdx1} mice (Figure 2A).

In order to determine how the number of Dclk1-positive cells was dynamically regulated during early pancreatic neoplasia, we quantified their relative abundance in normal pancreatic epithelium as well as in mPanIN and PDAC. In C^{iMist1} mice lacking oncogenic Kras, we observed minimal non-ciliary labeling for AcTub, but did identify Dclk1 expression in a small fraction (1–2 cells per field) of normal ductal epithelial cells. In contrast, we found that 10–20% of epithelial cells within ADM lesions and mPanIN1 expressed Dclk1 (Figure 2B–D). Although still much more frequent than in normal ductal epithelium, Dclk1-expressing cells became progressively less abundant in mPanIN2 and mPanIN3 lesions from KPC^{Pdx1} mice, and were rarely identified in invasive murine PDAC (Figure 2C,D). Combined analysis of Dclk1 and AcTub expression confirmed a high correlation between these two markers in ADM and early mPanIN, with progressive divergence in advanced mPanIN or invasive murine PDAC (Figure 3A). Notably, at both the late PanIN and PDAC stages we also observed increases in the abundance of stromal cells characterized by high levels of AcTub (Figure 3A).

To identify the cellular origin of AcTub+/ Dclk1+ epithelial cells in mPanIN, we performed lineage tracing experiments using $KC^{iMist1}Y$ mice. This analysis demonstrated that virtually all AcTub-positive mPanIN epithelial cells were also marked by YFP (Figure S1A), confirming that the AcTub+/ Dclk1+ cell subpopulation within KC^{iMist1} ADM and PanIN epithelium is acinar cell-derived.

AcTub+/DCLK1+ PanIN epithelial cells display characteristic tuft cell morphology

To determine whether AcTub+/Dclk1+ epithelial cells displayed classical tuft cell morphology, we performed additional analysis on pancreatic tissue from ADM- and PanIN-bearing KC^{iMist1} and KC^{Pdx1} mice, using both high-resolution DIC/confocal and transmission electron microscopy (TEM). As recently reviewed[19], tuft cells are specialized epithelial cells exhibiting abundant microtubule bundles in association with prominent apical microvilli. In ADM lesions identified in KC^{iMist1} mice, TEM confirmed the presence of a subpopulation of cells with apical microvilli (Figure 3B). These cells were interspersed among another minority cell population with acinar cell features (i.e. zymogen granules) and a more abundant population with duct cell features. TEM further confirmed the presence of low-abundance, morphologically discernible tuft cells in mPanIN lesions isolated from both KC^{iMist1} and KC^{Pdx1} mice (Figure 3B). In addition to prominent apical microvilli, the paucity of mucin granules in mPanIN tuft cells further distinguished them from the more predominant mPanIN cell type, in which these granules filled the entire apical cytoplasm. Combining high resolution DIC imaging with confocal microscopy, we were further able to confirm that tuft cell morphology and Dclk1 expression were tightly correlated (Figure 3C). Three-dimensional confocal imaging provided additional perspective on how these cells were spatially organized within mPanIN lesions, with areas of tuft cell clustering suggestive of specialized zones within each PanIN (Figure 3D; Supplemental Movie M1).

A subpopulation of cells in human PanIN and PDAC also display tuft cell features

In parallel to our analysis of murine PanIN and PDAC, we also analyzed the possible presence of a tuft cell-like subpopulation in human chronic pancreatitis, PanIN, and invasive PDAC. Immunostaining in human tissue was limited to AcTub, as multiple Dclk1 antibodies failed to generate reliable and reproducible labeling patterns. As in the case of murine PanIN and PDAC, human PanIN and PDAC lesions contained a minority cell population characterized by high level, cytoplasmic AcTub labeling (Figure S2A–C). To objectively

determine whether this pattern of labeling was associated with distinct tuft cell morphology, we surveyed multiple TEM fields from human PDAC and quantified maximal microvillus length for individual human PDAC cells. For comparison, a similar analysis was performed on murine PanIN. This analysis confirmed a dramatic bimodal distribution in maximal apical microvillus length in mPanIN, consistent with a subset of cells displaying classical tuft cell morphology. While median microvillus length in murine PanIN cells was less than 0.2 microns, mPanIN tuft cells displayed apical microvilli up to 4 microns in length (Figure S2F). In contrast, classical tuft cells were less evident on TEM imaging of invasive human cancer. Nevertheless, human PDAC cells also displayed a bimodal distribution in maximal microvillus length, with a subpopulation of cells displaying microvillus lengths in excess of 1 micron (Figure S2E,F). These findings suggest that while cells displaying classical tuft cell morphology are lost as human PanIN lesions progress to invasive cancer, some element of morphologic specialization may be retained.

AcTub+/DCLK1+ mPanIN cells display unique functional capacities

As a means to isolate and functionally characterize AcTub+/Dclk1+ PanIN tuft cells, we crossed KC^{iMist1} mice onto mTmG Cre reporter line, thereby generating $KC^{iMist1}G$ mice and $C^{iMist1}G$ control mice (Figure 4A,B). Using qRT-PCR to quantify *Dclk1* gene expression among FACS sorted mGFP+ cells, we confirmed a progressive increase in *Dclk1* expression during $Kras^{G12D}$-induced mPanIN formation (Figure 4C). Using GFP in combination with an antibody recognizing cell surface Dclk1[20], we further quantified the number of Dclk1+ cells during mPanIN formation by flow cytometry (Figure 4D, E). This revealed a 19-fold increase in the relative abundance of these cells in $KC^{iMist1}G$ mice compared to $C^{iMist1}G$ controls; this difference was further increased to 70-fold when PanIN formation was accelerated by the induction of chronic pancreatitis (Figure 4E).

In order to determine the functional correlates of cell surface Dclk1 expression, we isolated $GFP^{Br}/Dclk1^{HI}$ and $GFP^{Br}/Dclk1^{LO}$ cells from $KC^{iMist1}G$ mouse pancreas. Surprisingly, we also found that a fraction of GFP^{Br} cells isolated from $KC^{iMist1}G$ mice also had AcTub epitopes detectable on their cell surface (discussed further, below), correlating with their observed high levels of apical and cytoplasmic AcTub. In addition, the $GFP^{Br}/Dclk1^{HI}$ and $GFP^{Br}/AcTub^{HI}$ populations were largely overlapping, as assessed by flow cytometry. Based on the previous identification of Dclk1 as a marker of tumor stem cells[16, 21], we assayed FACS-isolated $GFP^{Br}/Dclk1^{LO}$, $GFP^{Br}/Dclk1^{HI}$ and $GFP^{Br}/AcTub^{HI}$ cells for clonogenic activity in a suspension culture system. In the absence of oncogenic Kras, the numbers of identified $GFP^{Br}/Dclk1^{HI}$ and $GFP^{Br}/AcTub^{HI}$ were extremely low, and no clonogenic activity was observed. In contrast, in the presence of oncogenic Kras, we observed an increased “PanIN sphere”-forming capacity in cells derived from either the $GFP^{Br}/Dclk1^{HI}$ or the $GFP^{Br}/AcTub^{HI}$ subpopulation relative to the $GFP^{Br}/DCLK1^{LO}/AcTub^{LO}$ fraction alone (Figure 4F and Table S1). Based on these findings, we conclude that morphologically distinct $GFP^{Br}/DCLK1^{HI}/AcTub^{HI}$ mPanIN epithelial cells display unique sphere-forming capacities similar to those displayed by cancer stem cells.

Cell surface labeling for AcTub and DCLK1 in human PDAC cells

Based on the identification of a functionally unique subpopulation of $GFP^{Br}/DCLK1^{HI}/AcTub^{HI}$ in murine PanIN, we subjected human pancreatic cancer cell lines as well as primary human tumor xenografts to cell surface labeling for AcTub and DCLK1, and in each case detected low-abundance (2–4% for cell lines; 3–9% for xenografts) $DCLK1^{HI}$ and $AcTub^{HI}$ cell populations. In these analyses, we found that greater than 90% of $AcTub^{HI}$ cells were also positive for DCLK1 (Supplemental Figure S3A). As in the case of $AcTub^{HI}$ cells identified in mPanIN, it was somewhat surprising to identify AcTub epitopes on the cell surface of human pancreatic cancer cells. We therefore employed a number of

techniques to confirm this finding, including immunofluorescent labeling and confocal imaging of fixed and unfixed cells, immunogold labeling followed by TEM, and cell surface protein biotinylation followed by immunoblot analysis. Each of these analyses confirmed the presence of enriched AcTub epitopes on the cell surface of AcTub^{HI} cells. In addition, AcTub^{HI} cells displayed increased expression of α-tubulin acetyltransferase (*ATAT1*; Figure S4A), and siRNA knockdown of ATAT1 reduced their relative abundance (Supplemental Figure S4B). Together, these findings strongly support the presence of cell surface AcTub epitopes on a subset of human pancreatic cancer cells.

The DCLK1^{HI}/AcTub^{HI} phenotype is shared by other pancreatic cancer stem cell populations

Based on our finding of enhanced clonogenic activity in the AcTub- and Dclk1-expressing mPanIN subpopulation, we hypothesized that AcTub^{HI}/DCLK1^{HI} PDAC cells might also display unique functional capacities. We used FACS analysis to compare the frequency of AcTub^{HI} labeling in cell populations expressing a series of previously published PDAC cancer stem cell markers, including CD133[7], CD24/CD44/ESA[4], and ALDH[5]. In these analyses, we found that cell populations labeling positive for either CD133 or CD24/CD44/ESA demonstrated up to 30-fold enrichment for AcTub^{HI} cells (Figure 5A,B). In contrast, we observed no enrichment and minimal overlap between the AcTub^{HI} and ALDH^{HI} populations (Figure 5B), suggesting that these two markers define independent PDAC cell subpopulations.

DCLK1^{HI}/AcTub^{HI} PDAC cells have tumor- and tumorsphere-initiating capabilities

We next determined whether DCLK1^{HI}/AcTub^{HI} PDAC cells were capable of clonogenic growth, similar to their mPanIN counterparts. Knowing that the DCLK1^{HI}/AcTub^{HI} and ALDH^{HI} phenotypes defined distinct and non-overlapping cell populations, and because ALDH^{HI} cells have been previously shown to display clonogenic and tumor-initiating capabilities, we directly compared DCLK1^{HI}/AcTub^{HI} and ALDH^{HI} for tumorsphere- and tumor xenograft-initiating capabilities. In these studies, only AcTub was used as a marker for DCLK1^{HI}/AcTub^{HI} cells, given the near-universal co-expression of DCLK1^{HI} within the AcTub^{HI} cell population. In tumorsphere-forming assays, AcTub^{HI} cells isolated from two different PDAC cell lines displayed an approximately 10-fold increase in sphere-forming efficiency compared to the more abundant AcTub^{LO}/ALDH^{LO} population, although they were ~50% less efficient than ALDH^{HI} cells (Figure 5C,D).

To determine the tumor initiating potential and growth potential of the AcTub^{HI} population *in vivo*, we sorted AcTub^{HI} and ALDH^{HI} cells from two human xenografts and implanted limiting dilutions of cells into immunodeficient mice. We injected either 100, 500, 1000 or 5000 cells per mouse and monitored tumor initiation over a series of 20 weeks. In these experiments, there was no tumor formation observed following injection of AcTub^{LO}/ALDH^{LO} cells. AcTub^{HI} cells formed tumors with a calculated tumor-initiating cell frequency of 1/1454 (95% confidence limits 1/3523 to 1/600), compared to 1/540 (95% confidence limits 1/1248-1/234) for ALDH^{HI} cells (Table 1). These findings suggest that that AcTub- and Dclk1-expressing human PDAC cells have cancer stem cell-like functional capabilities.

Tubulin acetylation and polymerization both regulate the clonogenic potential of DCLK1^{HI}/AcTub^{HI} PDAC cells

ATAT1 is the primary enzyme responsible for the acetylation of Tubulin on Lysine 40[22], while DCLK1 is a known regulator of tubulin polymerization[23]. Using quantitative RT-PCR, we determined that FACS-sorted AcTub^{HI}/DCLK1^{HI} and AcTub^{LO}/DCLK1^{HI} cells both had significant increases in *DCLK1* and *ATAT1* transcript abundance relative to

AcTub^{LO}/DCLK1^{LO} cells (Supplemental Figure S4A). To determine whether tubulin acetylation was required for tumor sphere initiation, we performed siRNA knockdown of *ATAT1* in two different human PDAC cell lines (AsPC1 and CFPAC). This resulted in a 3- to 7-fold reduction in sphere forming capacity compared to cells transfected with control siRNA (**p<0.01 for both AsPC1 and CFPAC) (Figure S4C,E). As an additional means to interrogate the apparent contribution of tubulin acetylation and polymerization to the clonogenic activity of AcTub^{HI}/DCLK1^{HI} cells, we also performed siRNA knockdown of both *DCLK1* and *Histone deacetylase 6* (*HDAC6*), the primary enzyme responsible for tubulin deacetylation [24–26]. For these experiments, we used bulk (unsorted) CFPAC cells and were able to achieve 75–80% reductions in target gene expression (Figure S4D). Knockdown of *HDAC6* led to a 1.5 fold increase in sphere formation (*p<0.05), consistent with tubulin acetylation exerting a positive influence on the clonogenic activity of PDAC cells (Supplemental Figure S4C). As in the case of *ATAT1*, *DCLK1* gene knockdown also resulted in a significant reduction in clonogenicity (*p<0.05) (Figure S4C).

Whole transcriptome analysis reveals gene and pathway enrichment in DCLK1^{HI}/AcTub^{HI} PDAC cells

As a means to identify genes and pathways potentially regulating the tumor-initiating capacities of DCLK1^{HI}/AcTub^{HI} PDAC cells, we performed whole transcriptome analysis on FACS-sorted cells from both the CFPAC and AsPC1 cell lines (Figure 5E,F). A complete listing of differentially expressed genes is provided in Table S2. Among 926 genes upregulated in DCLK1^{HI}/AcTub^{HI} cells from the CFPAC cell line and 921 genes similarly upregulated in DCLK1^{HI}/AcTub^{HI} cells from the AsPC1 cell line, 262 genes were upregulated in both cell lines (Figure 5E). Gene Ontology (GO) functional group enrichment analysis on these 262 genes defined transmembrane receptor activity as the most highly enriched functional group, with many other categories related to cell surface receptors also enriched (Figure 5F). Among genes found to be upregulated in DCLK1^{HI}/AcTub^{HI} cells were the tuft cell markers *TAS2R31*, *OR5A2* and *DCLK1* itself, as well as the Notch response genes *HES1*, *HES7* and *HEY1*. Additional genes found to be upregulated in DCLK1^{HI}/AcTub^{HI} cells included *ATAT1*, *ABL1* and *IGF1R*. We therefore performed additional functional studies investigating the role of these signaling pathways in regulating the relative abundance and/or the clonogenic capacities of DCLK1^{HI}/AcTub^{HI} PanIN and PDAC cells.

AcTub^{HI}/DCLK1^{HI} cell abundance is regulated by Notch signaling in both human PDAC and murine PanIN

Prior studies have implicated the Notch signaling pathway in the pathogenesis of pancreatic cancer[27, 28]. Using qRT-PCR, we confirmed upregulated expression of both *HES1* and *HEY1* in AcTub^{HI}/DCLK1^{HI} PDAC cells (Figure 6A). In order to determine the functional significance of Notch signaling in these cells, we forced Notch pathway activation in PDAC cells using retroviral vectors encoding the active, intracellular domain of either NOTCH1 (NICD1) or NOTCH3 (NICD3). Infection of PDAC cells with these retroviral vectors resulted in upregulated expression of *HES1* and *HEY1*, confirming effective pathway activation (Figure 6B). Notch pathway activation induced by ectopic expression of NICD3 also increased the expression of *ATAT1*. Expression of either NICD1 or NICD3 also dramatically increased the fraction of AcTub^{HI} PDAC cells (Figure 6C), while inhibition of Notch signaling using the γ-secretase inhibitor DAPT decreased the relative abundance of AcTub^{HI} cells (Figure 6D). Thus Notch signaling appears to be a potent regulator of AcTub^{HI}/DCLK1^{HI} cell abundance in human PDAC.

We next sought to determine whether the ability of Notch to regulate the abundance of AcTub^{HI}/DCLK1^{HI} cells *in vitro* might be correlated with a therapeutically relevant *in vivo*

effect. To achieve this, we compared the density of cells expressing Dclk1 in KPC^{Pdx1} mice treated with either vehicle or with the γ-secretase inhibitor MRK-003. In these studies, MRK-003 was delivered using an intermittent dosing regimen that effectively blocked PanIN progression[29]. In examining these tissues, *in vivo* γ-secretase inhibition was associated with a significant reduction in the number of Dclk1-expressing cells, expressed as the percentage of Dclk1-positive cells per PanIN (Figure 6E,F).

Inhibition of ABL and IGF1R reduce the sphere forming capacity of CFPAC cells

Microarray analysis also suggested upregulated expression of *ABL1* and *IGF1R* in $Dclk1^{HI}$/$AcTub^{HI}$ PDAC cells, a result further confirmed in by qRT-PCR (Figure S6A). We further confirmed a significant increase in *ABL1* transcript levels from FACS sorted GFP^{Br}/$DCLK1^{HI}$ relative to GFP^{Br}/$DCLK1^{LO}$ mPanIN cells from the $KC^{iMist1}G$ mouse model (Figure S6B). We therefore examined the effect of pharmacologic inhibition ABL1 on the clonogenic potential of bulk CFPAC cells. Using nilotinib to target ABL1, we observed a potent and dose-dependent reduction in tumorsphere formation mediated through a pro-apoptotic mechanism (Figure S6C–D) Similar effects were observed following inhibition of IGF1R signaling using linsitinib (data not shown).

CONCLUSIONS

In addition to identifying a novel and morphologically distinct subpopulation of tumor-initiating cells in human PDAC, these studies emphasize both morphologic and functional heterogeneity among epithelial cells within both murine and human PanIN. The current results complement a recent report demonstrating that distinct epithelial and mesenchymal subpopulations are generated following oncogenic Kras activation in adult acinar cells[30] and emphasize the need to consider PanIN lesions as a complex, multicellular tissue.

Prior studies have suggested that Dclk1 may mark tumor-initiating cells in a variety of tumor types[21, 31, 32]. In a recent report using the Apc^{Min} model, formal Cre/lox-based lineage tracing was employed to demonstrate that Dclk1-expressing cells within intestinal adenomas are responsible for the continuous production of tumor cell progeny, and that diphtheria toxin-mediated ablation of these cells results in tumor regression[33]. DCLK1 expression has previously been empirically demonstrated in both murine and human PanIN and PDAC. DCLK1 is also expressed by isolated cells within the pancreatic duct and islets of normal mouse pancreas, and prior studies have suggested that these non-neoplastic Dclk1-expressing pancreatic cells may also be associated with progenitor-like function[20].

While the cancer stem cell hypothesis has been most forcefully proposed as a feature of invasive malignancy, a number of recent studies have confirmed this principle to also be operative in several forms of pre-invasive neoplasia, including intestinal adenomas and skin papillomas[34]. We have demonstrated that $DCLK1^{HI}$/$AcTub^{HI}$ mPanIN cells display specialized morphology, unique patterns of gene expression and enhanced “PanIN sphere” forming ability. The ability to more formally implicate $DCLK1^{HI}$/$AcTub^{HI}$ mPanIN cells as PanIN stem cells is currently hindered by the fact that our current methodologies for lineage tracing and oncogenic Kras activation both require Cre/lox activity. Future progress in this area will depend on either the development of lineage tracing techniques using alternate DNA recombinases (e.g. Dre, Flp), or the development of non Cre/lox-based methods for Kras activation in murine pancreas.

Using whole transcriptome analysis, we identified multiple pathways that contribute to the cancer stem cell-like properties of $DCLK1^{HI}$/$AcTub^{HI}$ pancreatic cancer cells. Among these, tubulin acetylation itself appears to be required for optimal clonogenic function, establishing inhibition of ATAT1 or activation of HDAC6 as potential new therapeutic strategies. The

role of Notch signaling in pancreatic cancer is well established[27, 29, 35, 36], and recent studies have further implicated Notch in regulating pancreatic cancer stem cell function[37]; our studies suggest that this effect may in part be due to an influence on the relative size of the $DCLK1^{HI}/AcTub^{HI}$ subpopulation. Our studies also identified ABL1 and IGF1R to be highly expressed in $DCLK1^{HI}/AcTub^{HI}$ cells, complementing ongoing preclinical and clinical evaluation of ABL1 and IGF1R pathway inhibition as new forms of targeted therapy for pancreatic cancer[38, 39].

In summary, these studies suggest that both preinvasive and invasive pancreatic cancer may depend upon a unique subpopulation of DCLK1-expressing cells with cancer stem cell capabilities. As in the case of intestinal tumorigenesis[21], targeting this cell population may have therapeutic potential in the treatment and/or chemoprevention of pancreatic cancer.

Supplementary Material

Refer to Web version on PubMed Central for supplementary material.

Acknowledgments

The authors wish to thank Danielle Blake, Mara Swaim, Jeffrey Roeser, Anzer Habibulla, Dr. Hao Ho and Dr. Xiaogang Zhong for expert technical assistance and Dr. James Goldenring for many helpful discussions. We also thank Barbara Smith for expertise in TEM. TMA arrays were provided by the Hopkins Pathology Core. JMB is supported by the 2011 Pancreatic Action Network-AACR Pathway to Leadership Award and NCI 5F32 CA157044. JA is supported through the 5T32 CA126607 and the immixGroup Foundation Fellowship. ZR is supported by the Pancreatic Cancer Action Network-AACR Pathway to Leadership award. FM is supported by NIGMS T32GMO66691, 2012 Pancreatic Cancer Action Network-AACR Fellowship, in memory of Samuel Stroum, Grant Number 12-40-25-MCAL and Conquer Cancer Foundation Young Investigator Award 2012. WM is supported by R01 CA150142. SDL and AM were supported by NCI P01 CA134292. SDL was further supported by the Paul K. Neumann Professorship in Pancreatic Cancer at Johns Hopkins University.

References

1. Chen J, Li Y, Yu TS, McKay RM, Burns DK, Kernie SG, Parada LF. A restricted cell population propagates glioblastoma growth after chemotherapy. Nature. 2012; 488:522–6. [PubMed: 22854781]
2. Driessens G, Beck B, Caauwe A, Simons BD, Blanpain C. Defining the mode of tumour growth by clonal analysis. Nature. 2012; 488:527–30. [PubMed: 22854777]
3. Schepers AG, Snippert HJ, Stange DE, van den Born M, van Es JH, van de Wetering M, Clevers H. Lineage tracing reveals Lgr5+ stem cell activity in mouse intestinal adenomas. Science. 2012; 337:730–5. [PubMed: 22855427]
4. Li C, Heidt DG, Dalerba P, Burant CF, Zhang L, Adsay V, Wicha M, Clarke MF, Simeone DM. Identification of pancreatic cancer stem cells. Cancer Res. 2007; 67:1030–7. [PubMed: 17283135]
5. Rasheed ZA, Yang J, Wang Q, Kowalski J, Freed I, Murter C, Hong SM, Koorstra JB, Rajeshkumar NV, He X, Goggins M, Iacobuzio-Donahue C, Berman DM, Laheru D, Jimeno A, Hidalgo M, Maitra A, Matsui W. Prognostic significance of tumorigenic cells with mesenchymal features in pancreatic adenocarcinoma. J Natl Cancer Inst. 2010; 102:340–51. [PubMed: 20164446]
6. Olempska M, Eisenach PA, Ammerpohl O, Ungefroren H, Fandrich F, Kalthoff H. Detection of tumor stem cell markers in pancreatic carcinoma cell lines. Hepatobiliary Pancreat Dis Int. 2007; 6:92–7. [PubMed: 17287174]
7. Hermann PC, Huber SL, Herrler T, Aicher A, Ellwart JW, Guba M, Bruns CJ, Heeschen C. Distinct populations of cancer stem cells determine tumor growth and metastatic activity in human pancreatic cancer. Cell Stem Cell. 2007; 1:313–23. [PubMed: 18371365]
8. Hingorani SR, Petricoin EF, Maitra A, Rajapakse V, King C, Jacobetz MA, Ross S, Conrads TP, Veenstra TD, Hitt BA, Kawaguchi Y, Johann D, Liotta LA, Crawford HC, Putt ME, Jacks T, Wright CV, Hruban RH, Lowy AM, Tuveson DA. Preinvasive and invasive ductal pancreatic cancer and its early detection in the mouse. Cancer Cell. 2003; 4:437–50. [PubMed: 14706336]

9. Bardeesy N, Aguirre AJ, Chu GC, Cheng KH, Lopez LV, Hezel AF, Feng B, Brennan C, Weissleder R, Mahmood U, Hanahan D, Redston MS, Chin L, Depinho RA. Both p16(Ink4a) and the p19(Arf)-p53 pathway constrain progression of pancreatic adenocarcinoma in the mouse. Proc Natl Acad Sci U S A. 2006; 103:5947–52. [PubMed: 16585505]
10. Habbe N, Shi G, Meguid RA, Fendrich V, Esni F, Chen H, Feldmann G, Stoffers DA, Konieczny SF, Leach SD, Maitra A. Spontaneous induction of murine pancreatic intraepithelial neoplasia (mPanIN) by acinar cell targeting of oncogenic Kras in adult mice. Proc Natl Acad Sci U S A. 2008; 105:18913–8. [PubMed: 19028870]
11. Provost E, Wehner KA, Zhong X, Ashar F, Nguyen E, Green R, Parsons MJ, Leach SD. Ribosomal biogenesis genes play an essential and p53-independent role in zebrafish pancreas development. Development. 2012; 139:3232–41. [PubMed: 22872088]
12. Wang YJ, Bailey JM, Rovira M, Leach SD. Sphere-forming assays for assessment of benign and malignant pancreatic stem cells. Methods Mol Biol. 2013; 980:281–90. [PubMed: 23359160]
13. Seeley ES, Carriere C, Goetze T, Longnecker DS, Korc M. Pancreatic cancer and precursor pancreatic intraepithelial neoplasia lesions are devoid of primary cilia. Cancer Res. 2009; 69:422–30. [PubMed: 19147554]
14. Saqui-Salces M, Keeley TM, Grosse AS, Qiao XT, El-Zaatari M, Gumucio DL, Samuelson LC, Merchant JL. Gastric tuft cells express DCLK1 and are expanded in hyperplasia. Histochem Cell Biol. 2011; 136:191–204. [PubMed: 21688022]
15. Nam KT, O'Neal R, Lee YS, Lee YC, Coffey RJ, Goldenring JR. Gastric tumor development in Smad3-deficient mice initiates from forestomach/glandular transition zone along the lesser curvature. Lab Invest. 2012; 92:883–95. [PubMed: 22411066]
16. May R, Riehl TE, Hunt C, Sureban SM, Anant S, Houchen CW. Identification of a novel putative gastrointestinal stem cell and adenoma stem cell marker, doublecortin and CaM kinase-like-1, following radiation injury and in adenomatous polyposis coli/multiple intestinal neoplasia mice. Stem Cells. 2008; 26:630–7. [PubMed: 18055444]
17. Hofer D, Drenckhahn D. Cytoskeletal markers allowing discrimination between brush cells and other epithelial cells of the gut including enteroendocrine cells. Histochem Cell Biol. 1996; 105:405–12. [PubMed: 8781995]
18. Sureban SM, May R, Lightfoot SA, Hoskins AB, Lerner M, Brackett DJ, Postier RG, Ramanujam R, Mohammed A, Rao CV, Wyche JH, Anant S, Houchen CW. DCAMKL-1 regulates epithelial-mesenchymal transition in human pancreatic cells through a miR-200a-dependent mechanism. Cancer Res. 2011; 71:2328–38. [PubMed: 21285251]
19. Gerbe F, Legraverend C, Jay P. The intestinal epithelium tuft cells: specification and function. Cell Mol Life Sci. 2012; 69:2907–17. [PubMed: 22527717]
20. May R, Sureban SM, Lightfoot SA, Hoskins AB, Brackett DJ, Postier RG, Ramanujam R, Rao CV, Wyche JH, Anant S, Houchen CW. Identification of a novel putative pancreatic stem/progenitor cell marker DCAMKL-1 in normal mouse pancreas. Am J Physiol Gastrointest Liver Physiol. 2010; 299:G303–10. [PubMed: 20522640]
21. Nakanishi Y, Seno H, Fukuoka A, Ueo T, Yamaga Y, Maruno T, Nakanishi N, Kanda K, Komekado H, Kawada M, Isomura A, Kawada K, Sakai Y, Yanagita M, Kageyama R, Kawaguchi Y, Taketo MM, Yonehara S, Chiba T. Dclk1 distinguishes between tumor and normal stem cells in the intestine. Nat Genet. 2012; 45:98–103. [PubMed: 23202126]
22. Shida T, Cueva JG, Xu Z, Goodman MB, Nachury MV. The major alpha-tubulin K40 acetyltransferase alphaTAT1 promotes rapid ciliogenesis and efficient mechanosensation. Proc Natl Acad Sci U S A. 2010; 107:21517–22. [PubMed: 21068373]
23. Lin PT, Gleeson JG, Corbo JC, Flanagan L, Walsh CA. DCAMKL1 encodes a protein kinase with homology to doublecortin that regulates microtubule polymerization. J Neurosci. 2000; 20:9152–61. [PubMed: 11124993]
24. Castro-Castro A, Janke C, Montagnac G, Paul-Gilloteaux P, Chavrier P. ATAT1/MEC-17 acetyltransferase and HDAC6 deacetylase control a balance of acetylation of alpha-tubulin and cortactin and regulate MT1-MMP trafficking and breast tumor cell invasion. Eur J Cell Biol. 2012; 91:950–60. [PubMed: 22902175]

25. Bobrowska A, Paganetti P, Matthias P, Bates GP. Hdac6 knock-out increases tubulin acetylation but does not modify disease progression in the R6/2 mouse model of Huntington's disease. PLoS One. 2011; 6:e20696. [PubMed: 21677773]
26. Li G, Jiang H, Chang M, Xie H, Hu L. HDAC6 alpha-tubulin deacetylase: a potential therapeutic target in neurodegenerative diseases. J Neurol Sci. 2011; 304:1–8. [PubMed: 21377170]
27. Miyamoto Y, Maitra A, Ghosh B, Zechner U, Argani P, Iacobuzio-Donahue CA, Sriuranpong V, Iso T, Meszoely IM, Wolfe MS, Hruban RH, Ball DW, Schmid RM, Leach SD. Notch mediates TGF alpha-induced changes in epithelial differentiation during pancreatic tumorigenesis. Cancer Cell. 2003; 3:565–76. [PubMed: 12842085]
28. Doucas H, Mann CD, Sutton CD, Garcea G, Neal CP, Berry DP, Manson MM. Expression of nuclear Notch3 in pancreatic adenocarcinomas is associated with adverse clinical features, and correlates with the expression of STAT3 and phosphorylated Akt. J Surg Oncol. 2008; 97:63–8. [PubMed: 17918209]
29. Plentz R, Park JS, Rhim AD, Abravanel D, Hezel AF, Sharma SV, Gurumurthy S, Deshpande V, Kenific C, Settleman J, Majumder PK, Stanger BZ, Bardeesy N. Inhibition of gamma-secretase activity inhibits tumor progression in a mouse model of pancreatic ductal adenocarcinoma. Gastroenterology. 2009; 136:1741–9. e6. [PubMed: 19208345]
30. Rhim AD, Mirek ET, Aiello NM, Maitra A, Bailey JM, McAllister F, Reichert M, Beatty GL, Rustgi AK, Vonderheide RH, Leach SD, Stanger BZ. EMT and dissemination precede pancreatic tumor formation. Cell. 2012; 148:349–61. [PubMed: 22265420]
31. Vega KJ, May R, Sureban SM, Lightfoot SA, Qu D, Reed A, Weygant N, Ramanujam R, Souza R, Madhoun M, Whorton J, Anant S, Meltzer SJ, Houchen CW. Identification of the putative intestinal stem cell marker doublecortin and CaM kinase-like-1 in Barrett's esophagus and esophageal adenocarcinoma. J Gastroenterol Hepatol. 2012; 27:773–80. [PubMed: 21916995]
32. Sureban SM, May R, Ramalingam S, Subramaniam D, Natarajan G, Anant S, Houchen CW. Selective blockade of DCAMKL-1 results in tumor growth arrest by a Let-7a MicroRNA-dependent mechanism. Gastroenterology. 2009; 137:649–59. 659 e1–2. [PubMed: 19445940]
33. Nakanishi Y, Seno H, Fukuoka A, Ueo T, Yamaga Y, Maruno T, Nakanishi N, Kanda K, Komekado H, Kawada M, Isomura A, Kawada K, Sakai Y, Yanagita M, Kageyama R, Kawaguchi Y, Taketo MM, Yonehara S, Chiba T. Dclk1 distinguishes between tumor and normal stem cells in the intestine. Nat Genet. 2013; 45:98–103. [PubMed: 23202126]
34. Driessens G, Beck B, Caauwe A, Simons BD, Blanpain C. Defining the mode of tumour growth by clonal analysis. Nature. 2012; 488:527–30. [PubMed: 22854777]
35. De La OJ, Emerson LL, Goodman JL, Froebe SC, Illum BE, Curtis AB, Murtaugh LC. Notch and Kras reprogram pancreatic acinar cells to ductal intraepithelial neoplasia. Proc Natl Acad Sci U S A. 2008; 105:18907–12. [PubMed: 19028876]
36. Mazur PK, Einwachter H, Lee M, Sipos B, Nakhai H, Rad R, Zimber-Strobl U, Strobl LJ, Radtke F, Kloppel G, Schmid RM, Siveke JT. Notch2 is required for progression of pancreatic intraepithelial neoplasia and development of pancreatic ductal adenocarcinoma. Proc Natl Acad Sci U S A. 2010; 107:13438–43. [PubMed: 20624967]
37. Bao B, Wang Z, Ali S, Kong D, Li Y, Ahmad A, Banerjee S, Azmi AS, Miele L, Sarkar FH. Notch-1 induces epithelial-mesenchymal transition consistent with cancer stem cell phenotype in pancreatic cancer cells. Cancer Lett. 2011; 307:26–36. [PubMed: 21463919]
38. Ali Y, Lin Y, Gharibo MM, Gounder MK, Stein MN, Lagattuta TF, Egorin MJ, Rubin EH, Poplin EA. Phase I and pharmacokinetic study of imatinib mesylate (Gleevec) and gemcitabine in patients with refractory solid tumors. Clin Cancer Res. 2007; 13:5876–82. [PubMed: 17908982]
39. Rieder S, Michalski CW, Friess H, Kleeff J. Insulin-like growth factor signaling as a therapeutic target in pancreatic cancer. Anticancer Agents Med Chem. 2011; 11:427–33. [PubMed: 21492074]

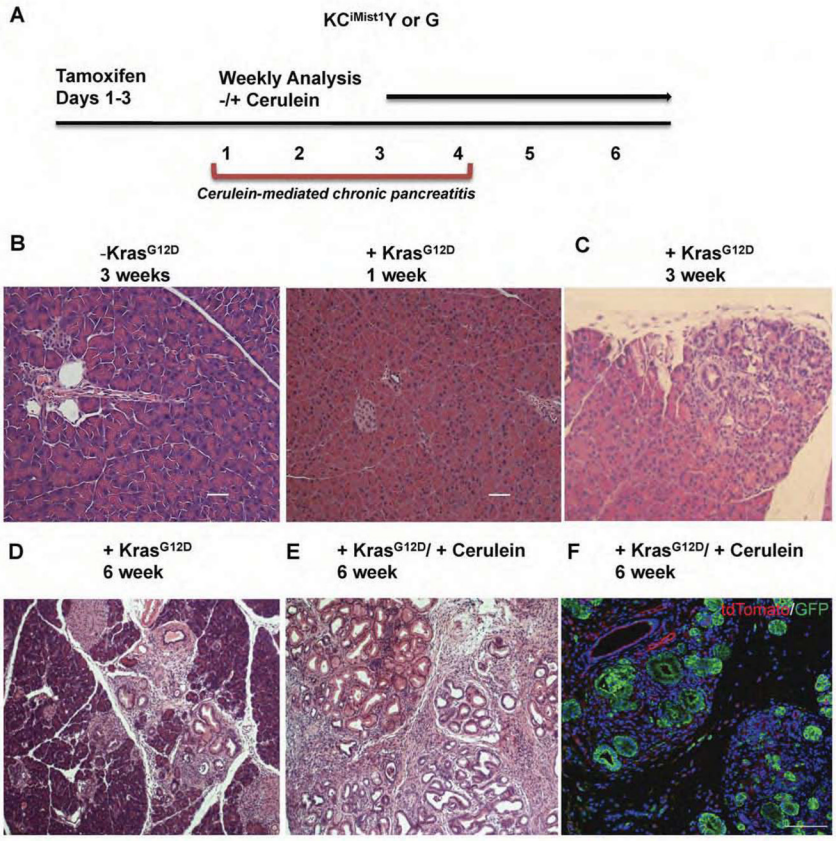

Figure 1. Histological analysis of mPanIN progression model after activation of oncogenic Kras in the acinar cell compartment

(A) Schematic illustrating tamoxifen induction of CreER^{T2} activity with and without concomitant cerulein-induced chronic pancreatitis in Mist1:CreER^{T2}; LSL-Kras; LSL-YFP (KC^{iMist1}Y) and Mist1:CreER^{T2}; LSL-Kras; mTmG (KC^{iMist1}G) mice. **(B–E)** Progressive PanIN formation with and without concomitant chronic pancreatitis. **(B)** No PanIN are detected in either the absence of Kras^{G12D} activation or 1 week following Kras^{G12D} activation. **(C)** Representative section depicting mPanIN three weeks after oncogenic Kras expression, at which point mPanINs typically occupy ~5% of cross sectional area. **(D)** Increased PanIN density 6 weeks following Kras^{G12D} activation, at which point mPanINs typically occupy ~10–15% of cross sectional area. **(E)** Accelerated PanIn formation following Kras^{G12D} activation in combination with cerulein-mediated chronic pancreatitis; PanIN lesions occupy greater than 70% of the pancreas. **(F)** Antibody labeling for GFP and tdTomato in pancreatic tissue harvested from KC^{iMist1}G mice confirms acinar cell origin of ADM and PanIN.

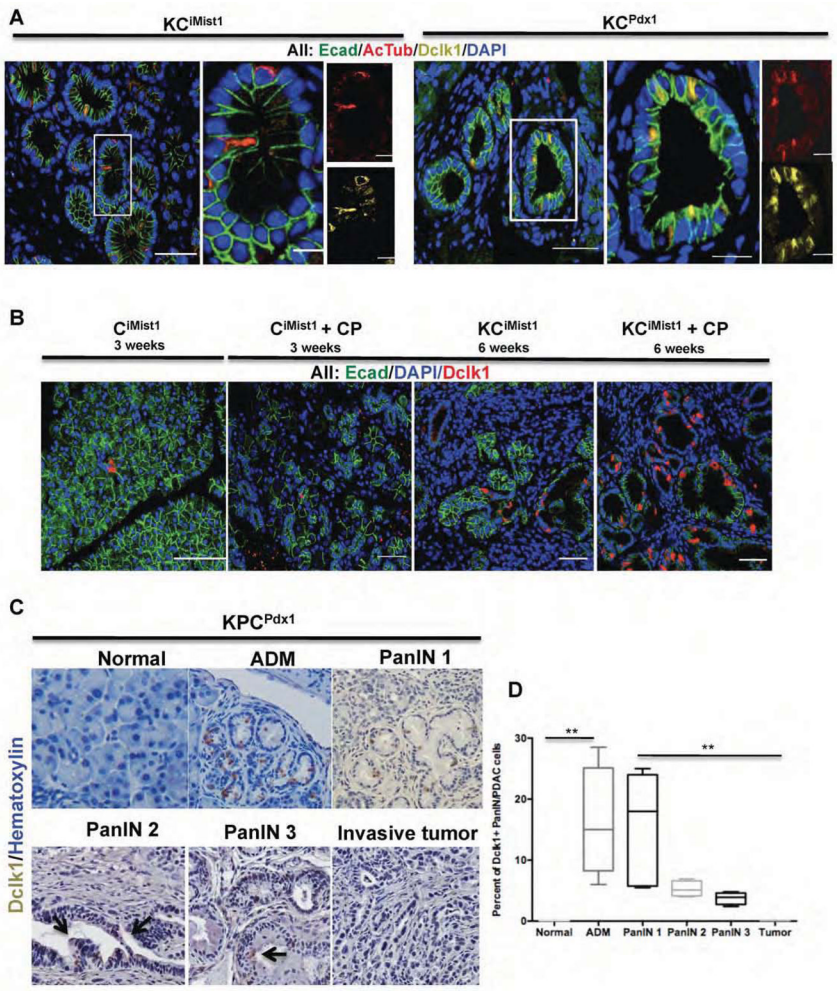

Figure 2. Dclk1 and AcTub label a distinct cell type in mPanIN

(A) Expression of E-cadherin (green), Dclk1 (yellow) and AcTub (red) in KC^{iMist1}+CP (6 weeks post tamoxifen) and KC^{Pdx1} (18 weeks old) mice. White boxes outline representative areas depicted at higher magnification in adjacent images. Note overlapping labeling for Dclk1 (yellow) and AcTub (red) in distinct subset of mPanIN epithelial cells. **(B)** Cerulein treatment increases the abundance of Dclk1-expressing cells within mPanIN. **(C)** Immunohistochemical analysis of Dclk1 expressing cells in KPC^{Pdx1} mice. (**D**) Dclk1 expressing cells are significantly increased in ADM, mPanIN and invasive PDAC relative to normal pancreatic ductal epithelium. Compared to PanIN1, however, the relative abundance of Dclk1-expressing cells progressively decreases in advanced PanINs and invasive PDAC (**p<0.01).

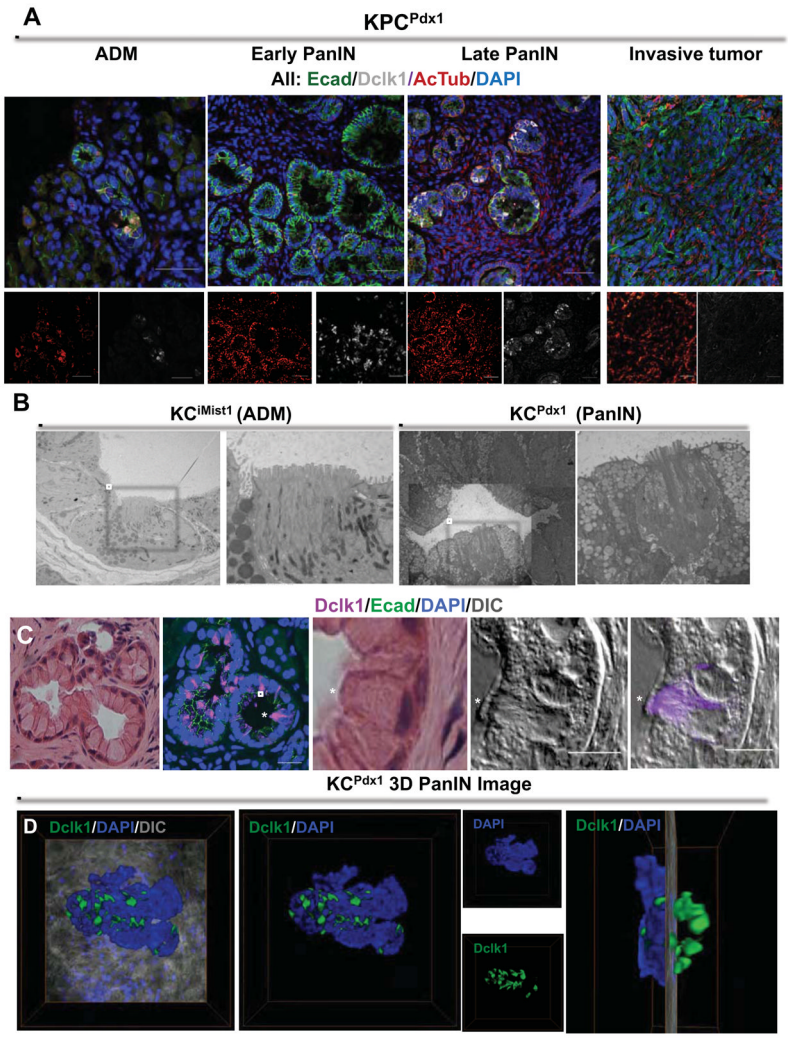

Figure 3. Dclk1- and AcTub-expressing PanIN cells display a tuft cell phenotype

(**A**) Immunoflourescent analysis of E-cadherin (green) Dclk1 (white) and AcTub (red) in ADM, early and late PanIN and invasive tumors from KPC^{Pdx1} mice. **(B)** Transmission electron micrograph depicting ADM (left) and mPanIN (right) from the KC^{iMist1} model. White boxes indicate cells with pronounced microvilli, shown at higher magnification in adjacent images.. (**C**) H&E staining on mPanIN from a 9 month old KC^{Pdx1} mouse. Confocal microscopy showing overlay of Dclk1 (purple) and E-cadherin (green). H&E and high-resolution confocal analysis of PanIN tuft cell (marked by *), displaying prominent apical microvilli and expressing Dclk1 (purple). (**D**) Three dimensional PanIN image from a 9 month old KC^{Pdx1} mouse showing spatial orientation of Dclk1 (green) positive cells. Right most image depicts 90 degree rotation of three-dimensional image, revealing clusters of Dclk1 expressing PanIN cells.

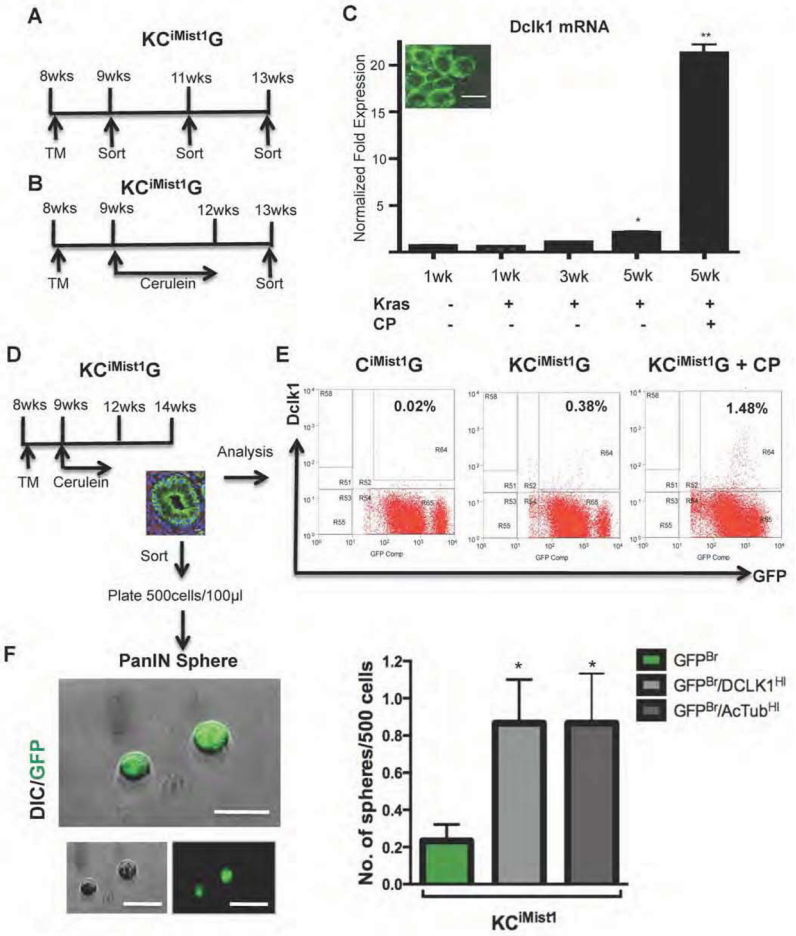

Figure 4. Dclk1 and AcTub cells show progenitor capability in preinvasive lesions

(**A,B**) Schematic outline of the sorting strategy to isolate eGFP+ cells at different time points after KC^{iMist1}G mice were treated with either tamoxifen alone (**A**) or tamoxifen and cerulein (**B**). (**C**) *Dclk1* mRNA levels significantly increase in FACS sorted GFP+ cells during mPanIN progression (**p<0.01). Inset shows imaging confirming membrane eGFP expression in isolated cells. (**D**) Sorting strategy for FACS-based isolation of eGFP+ cells from PanIN bearing KC^{iMist1}G + CP mice. To generate PanIN spheres, KC^{iMist1}G mice were treated with tamoxifen (TM) and cerulein, then left untreated for two weeks before the isolation of eGFP+ cells. (**E**) FACS analysis of KC^{iMist1}G + CP demonstrating dramatic increase in Dclk1-expressing cells. Percentages indicate fraction of all pancreatic cells comprising the Dclk1^{HI}/GFP^{Br} subpopulation. **(F)** PanIN-sphere formation by Dclk1^{HI}/GFP^{Br}, AcTub^{HI}/GFP^{Br}, and GFP^{Br} subpopulations. Dclk1^{HI}/GFP^{Br}, AcTub^{HI}/GFP^{Br}, and GFP^{Br} cells were FACS-sorted, plated at clonal density and cultured for seven days in low attachment plates. Graph indicates relative sphere-forming efficiency for different cell populations (*p<0.05 vs. GFP^{Br} control).

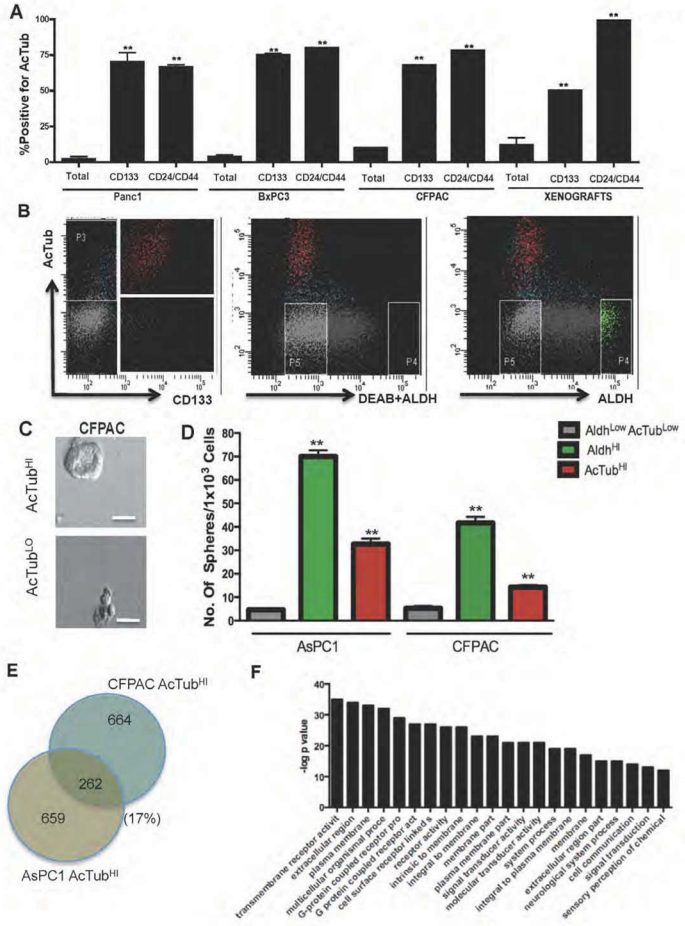

Figure 5. DCLK^{HI}/AcTub^{HI} cells are pancreatic cancer initiating cells

(**A**) Enrichment for cell surface AcTub labeling among CD133 or CD24/CD44/ESA positive cells in Panc1, BxPC3 and CFPAC cell lines and in two harvested human xenografts. Cells expressing CD133 or CD24/CD44/ESA are also enriched for expression of cell surface AcTub compared to the bulk cell population (**p<0.001). (**B**) FACS plots showing overlap of AcTub cell surface labeling with other published markers of pancreatic cancer stem cells, CD133 and ALDH. Significant overlap is observed for AcTub and CD133, but not for AcTub and ALDH (**C**) Tumor sphere derived from FACS sorted AcTub^{HI} cells from the CFPAC cell line (scale bar 50μm). (**D**) Graphical representation of *in vitro* tumor initiating capacity of AcTub^{HI}/DCLK1^{HI} subpopulations isolated from two different pancreatic cancer cell lines. The non-overlapping AcTub^{HI}/DCLK1^{HI} and ALDH^{HI} subpopulations formed significantly more spheres than the control AcTub^{LO}/ALDH^{LO} fraction (**p<0.01). **(E)** Whole transcriptome analysis on FACS-sorted AcTub^{HI} cells from both the CFPAC and AsPC1 cell lines. In these analyses, 926 genes were upregulated in AcTub^{HI} vs. AcTub^{LO} CFPAC cells and 921 genes were upregulated in AcTub^{HI} ASPC1 vs AcTub^{LO} cells. A total of 262 genes were upregulated in both CFPAC AcTub^{HI} and ASPC1 AcTub^{HI} cells. **(F)** Gene set enrichment analysis of 262 upregulated genes. The GO category “transmembrane receptor activity” was the most highly enriched functional group (p=1.322e-35), and many other groups related to cell surface receptors were similarly enriched. A complete listing of differentially expressed genes is provided in Table S2.

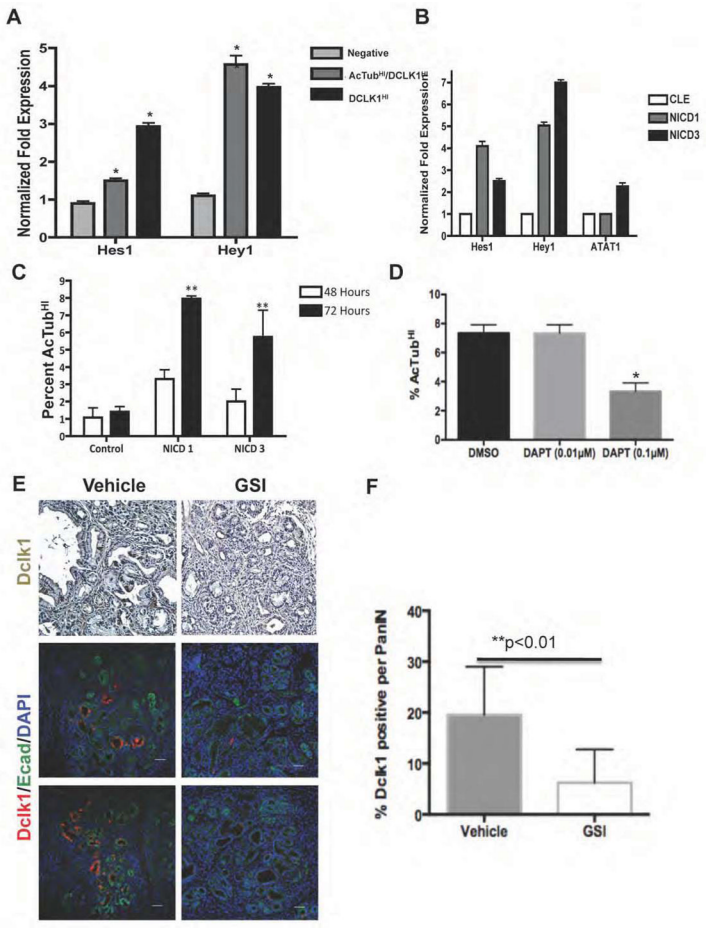

Figure 6. AcTub^{HI}/DCLK1^{HI} PDAC stem cell function is regulated by Notch

(**A**) Quantitative Real Time PCR confirming increased expression of *Hes1* and *Hey1* in FACS sorted AcTub^{HI}/DCLK1^{HI} cells. (**B**) Expression of NICD1 or NICD3 increases the expression of *Hes1*, *Hey1* and *ATAT1* mRNA levels. (**C**) Expression of NICD1 or NICD3 significantly increases the percentage of cells with detectable cell surface AcTub (**p<0.01). (**D**) Treatment of the CFPAC cell line with DAPT decreases the percentage of cells with cell surface AcTub labeling (*p<0.05). (**E**) Immunohistochemistry and immunoflourescent analysis of pancreatic tissue from vehicle-treated and γ-secretase inhibitor (MRK-300)-treated KPC^{Pdx1} mice. (**F**) Quantification of Dclk1 labeling shown in (E). In vivo inhibition of Notch signaling significantly reduces the fraction of mPanIN epithelial cells expressing Dclk1 (**p<0.01).

Table 1

Xenograft initiating capacity of FACS sorted AcTub^{HI} and ALDH^{HI} vs AcTub^{LO}/ALDH^{LO} cell populations.

Sorted Cell Population	No. Cells per injection	No. of tumors/No. of injections	TIC Frequency	P-value (vs. bulk)
Bulk	100	0/4	ND	ND
	500	0/4		
	1000	0/4		
	5000	0/4		
AcTub^{HI}	100	0/4	1/1454 (1/3523-1/600)	0.0000539
	500	1/4		
	1000	2/4		
	5000	4/4		
ALDH^{HI}	100	0/4	1/540 (1/1248-1/234)	0.00000045
	500	2/4		
	1000	4/4		
	5000	4/4		

Both AcTub^{HI} and ALDH^{HI} isolated cells had significantly increased xenograft initiating frequency compared to control cells (**p<0.001). TIC frequency was calculated using the Extreme Limiting Dilution Analysis software (Hu and Smyth, 2009).